NUMERICAL AIR QUALITY MODELLING IN COMPLEX URBAN ENVIRONMENT

A Thesis Submitted

In Partial Fulfillment of the Requirements

For the Degree of

MASTER OF TECHNOLOGY

In

Environmental Engineering and Management

By

JITENDRA KUMAR SINGH

to the

DEPARTMENT OF CIVIL ENGINEERING

INDIAN INSTITUTE OF TECHNOLOGY KANPUR

JULY, 2002

Certificate

This is to certify that the work contained in the thesis entitled 'Numerical Air Quality Modelling in Complex Urban Environment', by Jitendra Kumar Singh, has been carried out under our supervision and that this work has not been submitted elsewhere for a degree.

Mukesh Sharma 31/7/02

Dr. Mukesh Sharma
Associate Professor
Department of Civil Engineering

Shaktipada Ghorai 31/7

Dr. Shaktipada Ghorai
Assistant Professor
Department of Mathematics

INDIAN INSTITUTE OF TECHNOLOGY KANPUR

July, 2002

Abstract

To safeguard against air pollution hazards to health and property, air pollution control programs have to be undertaken. For any air-quality-management program to be rational, validated simulation models of diffusion of air pollutants have to be developed. Such diffusion models are the yardsticks for furnishing quantitative evaluation of concentrations of pollutants in the ambient air. In the present work, a three-dimensional, time dependent, air quality grid model, has been developed by numerically solving the atmospheric diffusion equation. This model integrates the mass-conservation equation, which includes advection, turbulent diffusion and source emissions. A wind field interpolation scheme is used to generate the mean transport winds from available measurements. While developing the scheme for numerical solution of the advection-diffusion equation, flux-limiter has been used so that the numerical advective flux function has the smoothing capabilities of the lower order scheme when it is necessary and the accuracy of the higher order scheme when it is possible. With the specified input parameters (wind speed, direction, mixing height, stability class, eddy diffusivities and source strength) the model is capable of predicting the gaseous pollutant concentration at any receptor point in the three-dimensional space. Also, it takes into account the emission source located anywhere in three-dimensional space.

The model was validated for PM_{10} concentrations. The model generally under predicted the PM_{10} levels, primarily due to incomplete emission source inventory of PM_{10}. The developed model was applied to various receptors on road-railway crossings in Kanpur city. Results indicate that concentration of CO and PM_{10} can peak 2-3 times higher than the national Ambient Air Quality Standards at some railway crossing receptors due to traffic congestions.

Keywords

Air quality models, advection, turbulent diffusion, flux-limiter, PM_{10}, CO

Dedicated

To

Papa

Acknowledgements

With utmost sincerity and pleasure, I express my overwhelming gratitude to Dr. Mukesh Sharma for his active supervision, consistent encouragement and unflagging moral and emotional support at every stage. I am grateful for his confidence in my abilities, which was instrumental in the success of this work.

I wish to express my gratitude to Dr. Shaktipada Ghorai and feel my fortune to get an opportunity of working with him. He has always, without exception, spared his precious time for me, whenever I needed his help and guidance. His unique friendly way of discussions will always remain a source of inspiration for me.

I consider myself fortunate for having been student of IIT Kanpur and would like to thanks other professors for their guidance and Mishra ji and R.B.Lal ji for their invaluable help during the experiments.

Thanks are due to the help and providing assistance by Central Pollution Control Board, Kanpur during the experiments.

I am also thankful for Professor D.C.Keim, Weather Scientist, CSA Agricultural University for providing the required meteorological data and useful information.

I remember lovable and pleasant company of my friends, as their help and guidance at all time during my stay at IIT Kanpur has enabled me to tide over all the difficulties. I deeply cherish my association with my friends and juniors.

JITENDRA KUMAR SINGH

Contents

List of Figures

List of Tables

1. Introduction

1.1 Air Quality Modelling

To safeguard against air pollution hazards to health and property, air pollution control programs have to be undertaken. The concentration of a pollutant at the points of significance from community point of view, depends on source strength and the dispersal capacity of the intervening atmosphere. Hence, for any air-quality-management program to be rational, simulation models of diffusion of air pollutants have to be developed. Such diffusion models are the yardsticks for furnishing quantitative evaluation of concentrations of pollutants in the ambient air.

Mathematical diffusion models can be used as an aid to decision making in air pollution control and for city and regional planning. These models can be used in long-range air-source management programs for the evaluation of future air quality with regard to increased population. They can be used to evaluate the effectiveness of individual control or abatement procedures for a given source or a combination of sources. Models may also be useful for determining most suitable locations for pollution-causing industrial units as also that of sampling stations used to monitor air pollution levels. It may be possible to use short-range predictions of meteorological variables with appropriate source information to produce maps of expected air pollution concentrations in a few minutes with the help of a digital computer. These would be an aid in initiating immediate measures necessary to achieve desired air quality levels.

A central practical problem is the prediction of the average concentration of a pollutant, at a specified location, which results from the contributing sources whose emission rates and locations are prescribed. This problem is solved only after a variety of simplifying assumptions are made. The understanding of the limitations that are imposed by these simplifications is necessary to evaluate the circumstances under which the various methods apply.

The basis of most mathematical descriptions of atmospheric diffusion is the "K- theory" equation, which relates the concentration of a substance, as a function of position and time, with the action of average wind flows and turbulence.

The K- theory equation in the absence of chemical reaction and source terms is

$$\frac{\partial c}{\partial t} + \frac{\partial (uc)}{\partial x} + \frac{\partial (vc)}{\partial y} + \frac{\partial (wz)}{\partial z} = \frac{\partial}{\partial x}\left(K_{xx}\frac{\partial c}{\partial x}\right) + \frac{\partial}{\partial y}\left(K_{yy}\frac{\partial c}{\partial y}\right) + \frac{\partial}{\partial z}\left(K_{zz}\frac{\partial c}{\partial z}\right) \qquad (1.1)$$

Here,

c	concentration of the pollutant
u,v,w	wind speeds in the x,y and z directions respectively
K_{xx}, K_{yy} and K_{zz}	coefficients, known as eddy diffusivities
x,y,z	distances along the Cartesian axes
t	time

The terms on the right hand side in Equation (1.1) represent diffusion due to turbulence; while on the left hand side (except the first term) represent the advection.

To obtain the classic Gaussian plume model (analytical solution of Equation 1.1), the following assumptions are made:

- The solution is time invariant
- The wind speed is not a function of position
- The diffusivities are not functions of position
- Diffusion in the x-direction is insignificant compared to mean flow in that direction.

With these assumptions, the equation has an analytical solution, which expresses the concentration as a Gaussian or Normal distribution in the y and z directions.

While the Gaussian equations have been widely used for atmospheric diffusion calculations, the lack of ability to include changes in wind speed with height and nonlinear chemical reactions limits the situations in which they may be used. Applications of simple Gaussian models, under complex urban conditions have been questioned by several researchers (Budianski, 1980). The atmospheric diffusion equation provides a more general approach to atmospheric diffusion calculations than the Gaussian models, since the Gaussian models have been shown to be special cases of that

equation when the wind speed is uniform and the eddy diffusivities are constant. To overcome the limitations of application of Gaussian model in complex situations, the above described advection- diffusion equation has been solved numerically (Numerical Models).

The key problem in the use of Equation (1.1) is to choose the functional forms of the wind speeds, u, v, w and the eddy diffusivities, K_{xx}, K_{yy}, K_{zz}, for the particular situation of interest.

Appendix A shows available methods and formulations to estimate variations in wind speeds and eddy diffusivities with height and stability conditions.

Here, Eulerian formulation approach is being used for the numerical solution of the Equation (1.1). In this formulation, a fixed coordinate system, or grid, is laid out over the entire region of interest. The concentration of a pollutant in each cube of the grid is then calculated by solving the equation, using numerical methods and with the help of a digital computer, over a series of small time. In the grids, which contain sources, a source term is added to the right side of the K- theory equation. This approach is most useful for situations in which there are multiple sources or for which predicted concentrations are needed for the entire region.

1.2 Thesis Objectives

In view of the above discussions concerning application of Gaussian models under complex urban settings, the objectives of the thesis can be worded as under

1. To develop a three-dimensional time dependent numerical model for dispersion of air pollutant under complex urban settings including traffic congestion/stagnation.
2. To apply the developed model for prediction of pollutant concentration at traffic intersections in the city of Kanpur characterized by complex criss-cross network of road and railway line with multiple level crossings.

2. Literature Review

2.1 Vehicular Source Air Quality Modelling

In most of the Indian cities, traffic is the most important source of air pollution, and pollution from major roads is also important in suburban and rural areas. Vehicular dispersion models are therefore essential computational tools in modern urban planning.

Most frequently, due to their simplicity and direct applicability for estimates on a local scale, various versions of the Gaussian line source model have been used for dispersion evaluations from a road. Such models include GM (Chock, 1978), GFLSM (Luhar and Patil, 1989), IITLS (Goyal and Krishna, 1999) and CAR-FMI (Harkonen et al., 2001).

A simple line source (GM) model was proposed by Chock (1978) to discuss the downwind dispersion of pollutants near the roadway. It required only simple calculations and was found to be potentially more accurate than the existing Gaussian models, especially under adverse meteorological conditions.

Because of the infinite line source assumption, the GM model is applicable to a situation where the upwind segment of the road (measured from the perpendicular line drawn from the receptor) is at least three times the distance between the receptor and the road. Hence, the GM model overpredicts the concentration by a considerable amount if the above constraint is not satisfied (Luhar and Patil, 1989). This constraint can be handled by using the HIWAY-2 model (Peterson, 1980), but its performance is not as good as that of GM model.

In HIWAY-2 and CALINE-4 models, the concentrations predicted by Gaussian line source equation are solved by a numerical procedure. This procedure divides the road into a series of elements, from which incremental concentrations are then computed and summed up. Both models allow for a finite mixing height in the computations.

The GFLSM model (Luhar and Patil, 1989) utilizes an analytical solution of the Gaussian equation for a finite line source, this solution allows for any wind direction

with respect to the road. The analytic solution has been originally derived from Gaussian formulae similar to, for instance, the HIWAY-2 and CALINE-4 models, except that the mixing height has been assumed to be infinite.

Luhar and Patil (1989) presented evaluation of road dispersion models against experimental data sets. They presented testing of the GFLSM model, including data for fine particulate matter. The particulate matter data set was produced at a location on an expressway in NewYork, and also contained traffic counts and meteorological measurements. The model clearly overpredicted the measured fine particulate matter concentrations.

Another line source model, based on Gaussian formulation, has been developed by IIT Delhi (IITLS model, Goyal and Krishna, 1999), in which improvements have been made in the calculation of source strength at major intersections in a city by considering the vehicular speed.

Harkonen et al. (2001) evaluated the CAR-FMI model against measurement near a major road. They compared the measured concentration data with the prediction of the road network dispersion model. They had also analyzed the difference between model predictions and measured data in terms of meteorological parameters.

Industrial Source Complex Short-Term (ISCST 3) model is a regulatory model of USEPA (454/B-95-003a-c). It is primarily used for point sources of industrial origin. However, like other Gaussian models, this can only calculate steady state concentrations with smallest time resolution being one hour.

All the above-discussed models are based on the Gaussian formulation. Under a complex urban setting, the source location varies in three-dimensional space. Also, the receptor point of our interest may be anywhere in the space up to a reasonable height. Variation of wind speed and eddy diffusivities must be taken into account for such cases. With the limitations in the applicability of these models under different conditions, as discussed earlier, development of a numerical algorithm is needed to solve the basic transport equation in Eulerian grid models and such a model is developed in chapter 3.

3. Development of Numerical Air Quality Model

3.1 Numerical Method for Solving the Advection-Diffusion Problem

The objective of this chapter is to devise a scheme for the solution of Equation 1.1 of the atmospheric diffusion, which has been reproduced here for convenience.

$$\frac{\partial c}{\partial t}+\frac{\partial}{\partial x}(uc)+\frac{\partial}{\partial y}(vc)=\frac{\partial}{\partial x}\left(k_{xx}\frac{\partial c}{\partial x}\right)+\frac{\partial}{\partial y}\left(k_{yy}\frac{\partial c}{\partial y}\right)+\frac{\partial}{\partial z}\left(k_{zz}\frac{\partial c}{\partial z}\right) \qquad (3.1.)$$

to predict the time dependent concentration of air pollutants in three dimension. Here c is the concentration of the pollutant, u and v are the horizontal wind velocities and k_{xx}, k_{yy} and k_{zz} are the diffusivities. There will be source term and initial and boundary conditions with the problem.

3.1.1 Advection Scheme

To analyse the various numerical advection schemes, we first consider one-dimensional wave equation

$$\frac{\partial c}{\partial t}+\frac{\partial}{\partial x}(uc)=0 \qquad (3.2)$$

Consider grid points k-1, k and k+1. k-1/2 and k+1/2 denote the positions between them respectively.

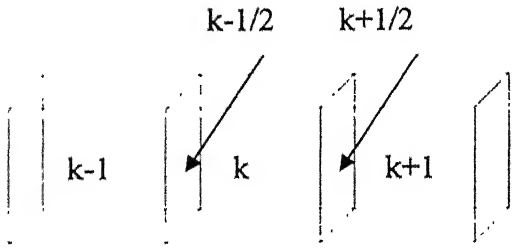

Integrating equation (3.2) between $x_{k-1/2}$, $x_{k+1/2}$ and t_n, $t_{n+1}=t_n+\Delta t$ gives

$$c_k^{n+1} = c_k^n - R\left(F_{k+1/2}^n - F_{k\ 1/2}^n\right) \tag{3.3}$$

where R=Δt/Δx. Here F denotes the flux through the respective faces. In the case of *upwind scheme*, $F_{k+1/2}^n$ is replaced by

$$F_{k+1/2}^n = \frac{1}{2}u\left(c_{k+1}^n + c_k^n\right) - \frac{1}{2}|u|\left(c_{k+1}^n - c_k^n\right) \tag{3.4}$$

This means if u>0, then $F_{k+1/2}^n = u\,c_k^n$ and if u<0, $F_{k+1/2}^n = u\,c_{k+1}^n$. Though the scheme has nice property, it is a lower order scheme since it is only first order in space. Thus the scheme suffers from excessive numerical diffusion.

Hence high-resolution schemes should be applied here. High-resolution schemes are generally second-order accurate on smooth sections of the solution, nonoscillatory and capable of resolving discontinuities in the solution. Flux-Limiter methods are being applied for this purpose. The numerical flux function is written as

$$F_{k+1/2}^n = F_{L\,k+1/2}^n + \phi_{k+1/2}^n\left[F_{H\,k+1/2}^n - F_{Lk+1/2}^n\right] \tag{3.5}$$

where F_L and F_H are numerical flux functions of a lower order scheme and a higher order scheme respectively and $\phi_{k+1/2}^n$ is a coefficient (called as flux-limiter) that is yet to be defined. It is to be noted that the flux in upwind scheme given in equation (3.4) is lower order. The idea is to develop a scheme where the numerical flux function has the smoothing capabilities of the lower order scheme when it is necessary and the accuracy of the higher order scheme when it is possible. Thus ϕ is being defined such that it is near 1 on smooth sections of the solution ($F_{k+1/2}^n$ will be approximately equal to $F_{H\,k+1/2}^n$) and near 0 on sections of the solution that contain steep gradient or discontinuities ($F_{k+1/2}^n$ will be approximately equal to $F_{Lk+1/2}^n$).

And, Equation (3.5) can also be written as

$$F^n_{k+1/2} = F^{\ n}_{H\,k+1/2} - \left(1-\phi^n_{k+1/2}\right)\left[F^{\ n}_{H\,k+1/2} - F^{\ n}_{L\,k+1/2}\right] \tag{3.6}$$

Thus the flux limiter methods can be viewed either as perturbing the flux of a lower order scheme or perturbing the flux of a higher order scheme.

We already know that upwind flux can be taken as F_L. For the higher order flux, following schemes can be used successfully.

The first one is called Lax- Wendroff scheme:

$$F^{\ n}_{H\,k+1/2} = uc^n_k + \frac{1}{2}u\left(1-u\tilde{R}\right)\delta_+ c^n_k \tag{3.7}$$

where $\delta_+ c^n_k = c^n_{k+1} - c^n_k$.

The second scheme is called Mid-Point scheme where the flux is given by

$$F^{\ n}_{H\,k+1/2} = \frac{1}{2}u\left(c^n_k + c^n_{k+1}\right) \tag{3.8}$$

There are many ways to accomplish the goal of achieving ϕ near 1 in smooth regions and 0 near discontinuities. A common approach is to write

$$\phi^n_{k+1/2} = \phi\left(\theta^n_k\right),$$

where θ^n_k is a smoothness parameter. We take

$$\theta^n_k = \frac{\delta_- c^n_k}{\delta_+ c^n_k}, \tag{3.9}$$

where $\delta_- c^n_k = c^n_k - c^n_{k-1}$.

θ^n_k is used to measure the smoothness of the solution, because when the solution is not changing much, it will be approximately 1, and when the solution is changing a significant amount, it will be very different from 1.The function ϕ is chosen such that the numerical scheme satisfy some desirable properties. These will be satisfied if we require ϕ to satisfy

$$0 \le \frac{\phi(\theta)}{\theta} \le 2 \quad \text{and} \quad 0 \le \phi(\theta) \le 2 \tag{3.10}$$

for all θ. Some of the choices for limiter functions that are in the literature include the following:

Superbee Limiter:

$$\phi(\theta) = \max\{0, \min[1, 2\theta], \min[\theta, 2]\} \tag{3.11}$$

Van Leer Limiter:

$$\phi(\theta) = \frac{\theta + |\theta|}{1 + |\theta|} \tag{3.12}$$

The above numerical scheme can easily be extended to two dimensions. In this case, we consider

$$\frac{\partial}{\partial t}c + \frac{\partial}{\partial x}(uc) + \frac{\partial}{\partial y}(vc) = 0 \tag{3.13}$$

Integrating the above equation with respect to t from t_n to t_{n+1}, from $x_{j-1/2}$ to $x_{j+1/2}$ with respect to x and from $y_{k-1/2}$ to $y_{k+1/2}$ with respect to y, we get

$$c_{j,k}^{n+1} = c_{j,k}^{n} - R_x\left[P_{j+1/2,k}^{n} - P_{j-1/2,k}^{n}\right] - R_y\left[Q_{j,k+1/2}^{n} - Q_{j,k-1/2}^{n}\right] \tag{3.14}$$

Where $R_x = \Delta t/\Delta x$ and $R_y = \Delta t/\Delta y$. Here P and Q are the fluxes in the x and y directions respectively. Proceeding as before, we write

$$P_{j+1/2,k}^{n} = P_{H\,j+1/2,k}^{\ n} + \phi_{j+1/2,k}^{n}\left[P_{H\,j+1/2,k}^{\ n} - P_{L\,j+1/2,k}^{\ n}\right]$$

where ϕ is the limiter function, P_L and P_H denote the fluxes based on lower and higher order schemes. Similarly we write the flux along the y- direction also. The same scheme is obviously generalized to three dimensions.

3.1.2 Diffusion Scheme

Again, first we consider a simple one-dimensional equation of the form

$$\frac{\partial c}{\partial t} = \frac{\partial}{\partial x}\left(K\frac{\partial c}{\partial x}\right), \tag{3.15}$$

Where K is the diffusivity constant. Integrating the above equation from t_n to $t_{n+1/2}$ for t and from $x_{j-1/2}$ to $x_{j+1/2}$ for x, we get

$$\frac{\Delta x}{\Delta t}\left[c_j^{n+1} - c_j^n\right] = K_{j+1/2}\left.\frac{\partial c}{\partial x}\right|_{j+1/2} - K_{j-1/2}\left.\frac{\partial c}{\partial x}\right|_{j-1/2}. \tag{3.16}$$

Expanding the term on the right hand side further, we get

$$\frac{\Delta x}{\Delta t}\left[c_j^{n+1} - c_j^n\right] = K_{j+1/2}\frac{c_{j+1}^{n+1} - c_j^{n+1}}{\Delta x} - K_{j-1/2}\frac{c_j^{n+1} - c_{j-1}^{n+1}}{\Delta x} \tag{3.17}$$

This is an implicit scheme, since the time step for the explicit scheme is very small. The above equation can be written as

$$a_j c_j^{n+1} = c_j^n + a_{j+1} c_{j+1}^{n+1} + a_{j-1} c_{j-1}^{n+1} \tag{3.18}$$

where

$$a_{j+1/2} = K_{j+1/2}\frac{\Delta t}{\Delta x^2}$$

$$a_{j-1/2} = K_{j-1/2}\frac{\Delta t}{\Delta x^2}$$

and

$$a_j = 1 + a_{j+1/2} + a_{j-1/2}$$

The above technique can be generalized to two and three dimensions in obvious way.

3.1.3 Solution Method

The Equation (3.1) in three dimensions is discretized as (using the techniques of the previous sections)

$$a_{i,j,k}\, c^{n+1}_{i,j,k} = c^{n}_{i,j,k} - R_x \left[F^{n}_{i+1/2,j,k} - F^{n}_{i-1/2,j,k}\right] - R_y \left[G^{n}_{i,j+1/2,k} - G^{n}_{i,j-1/2,k}\right]$$
$$+ a_{i+1/2,j,k}\, c^{n+1}_{i+1,j,k} + a_{i-1/2,j,k}\, c^{n+1}_{i-1,j,k} + a_{i,j+1/2,k}\, c^{n+1}_{i,j+1,k} + a_{i,j-1/2,k}\, c^{n+1}_{i,j-1,k}$$
$$+ a_{i,j,k+1/2}\, c^{n+1}_{i,j,k+1} + a_{i,j,k-1/2}\, c^{n+1}_{i,j,k-1} \qquad (3.19)$$

Where R's and a's have expressions similar to those of the previous sections. In the scheme, advection is treated explicitly and diffusion is treated implicitly. The above equations on the mesh are solved using iterative techniques such as Gauss –Seidel method with relaxation.

3.2 Validation of the Code for Advection Algorithm

3.2.1 Standard Cone Test

To verify the advection scheme using a limiter, the classic cone test in a solid body rotational flow-field has been used. The flow-field velocities are defined over a 100x100-grid cell domain:

$$u = -\omega y \text{ and } v = \omega x \text{ with } \omega = 0.1.$$

The initial condition has a cone of radius 15 grids and height of 5, above a background of base value 1. The cone is centered at (50,75). This test is often used to investigate the accuracy of advection schemes (Clappier, A., 1998). It is important to note that this rotational flow-field is monodimensionally divergence free

$$\left(\frac{\partial u}{\partial x} = \frac{\partial v}{\partial y} = 0 \right)$$

During this test, the cone should rotate around the domain, keeping the same shape.

3.2.2 Suitability of the Limiter and High Order Schemes

To verify the best suitability of the limiter and high order schemes, the combinations of the earlier mentioned limiters with high order schemes has been taken one by one and standard cone test is applied. The combination, which preserves the shape of the cone at most with less reduction in peak is taken to be the best and is applied here.

Here, we find that the Van-leer limiter with lax-Wendroff scheme fulfills the requisites better in comparison to the others. The cone test results for one full rotation in the horizontal plane, applied to the various combinations are as given here:

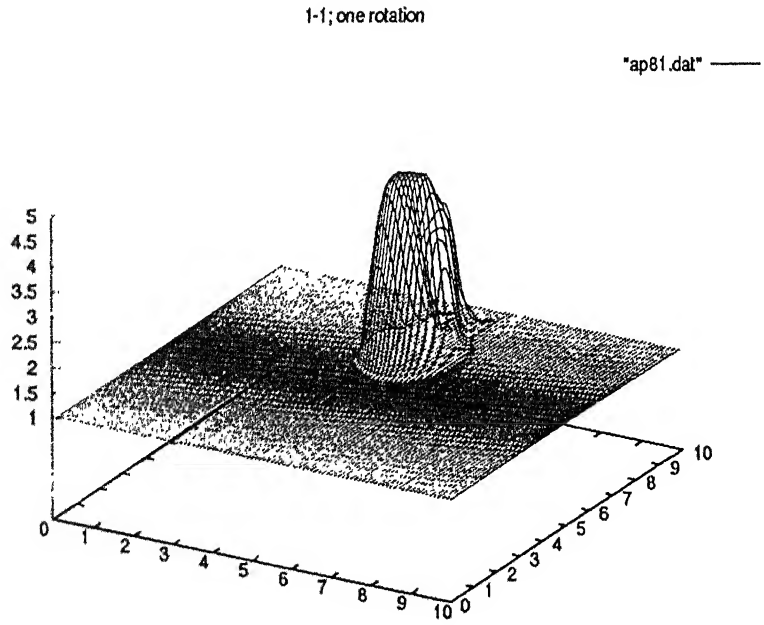

Figure 3.1 Mid-point Scheme; Van-leer Limiter

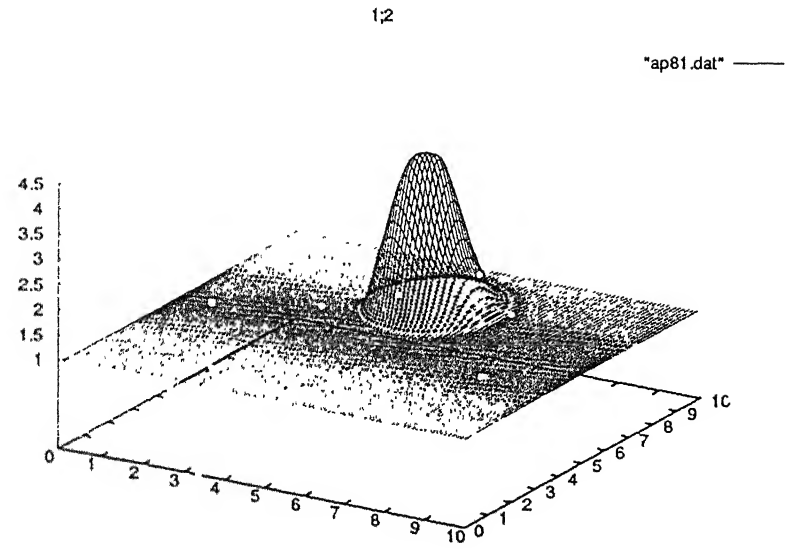

Figure 3.2 Lax-Wendroff Scheme; Van-leer Limiter

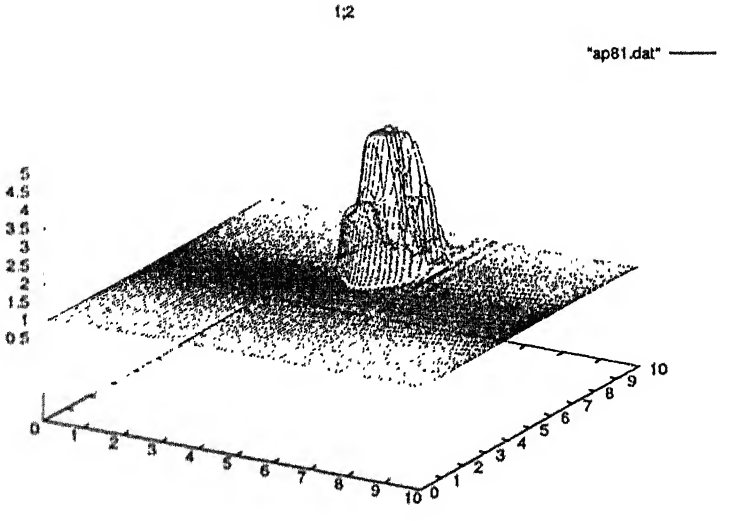

Figure 3.3 Mid-point Scheme; Superbee Limiter

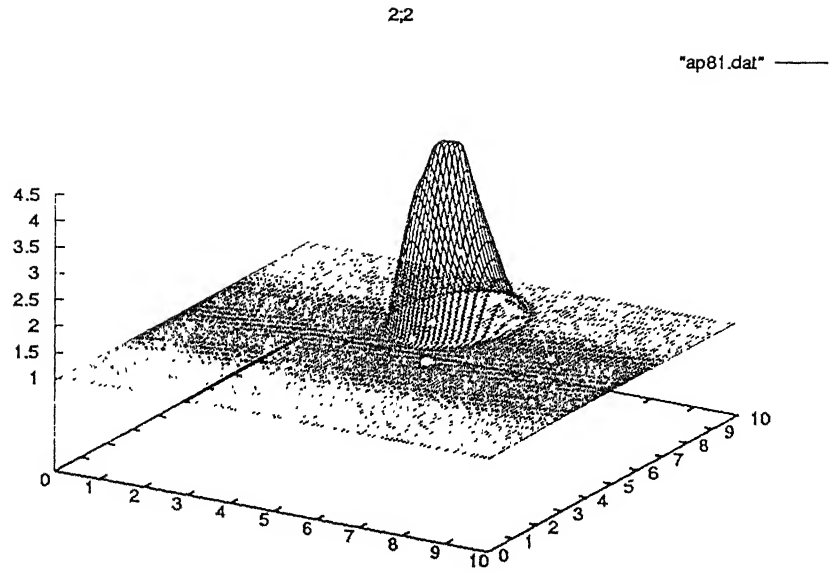

Figure 3.4 Lax-Wendroff Scheme; Superbee Limiter

3.2.3 Cone Test for the Lower Order Scheme

As discussed earlier, lower order scheme is the Upwind Scheme. When cone test is applied for the scheme, there is much reduction in the peak with deformation in the basic shape of the cone.

The shape is no more preserved after one and two rotations of the cone. Also, the peak of the cone has reduced considerably (sixty percent reduction after one rotation and seventy five percent reduction after two rotations), thus restricting for the use of the lower order scheme.

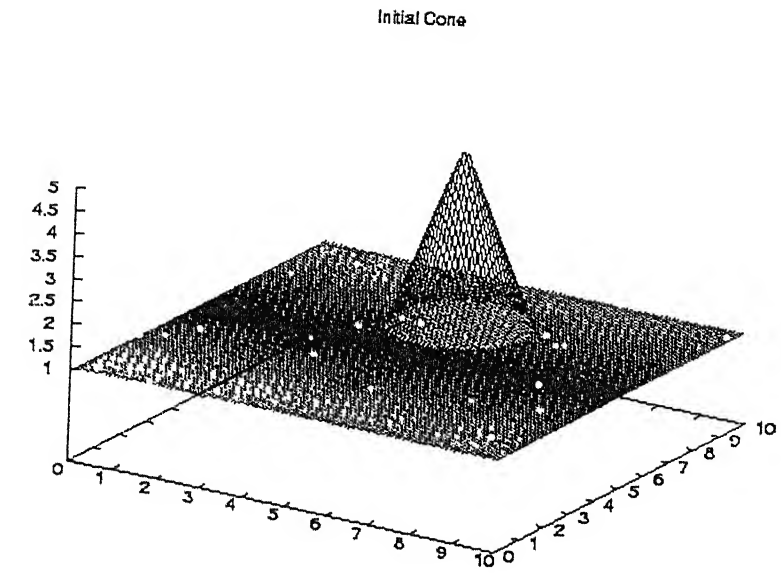

Figure 3.5 Initial Cone (Centre at 5,7.5 and radius 1.5 units)

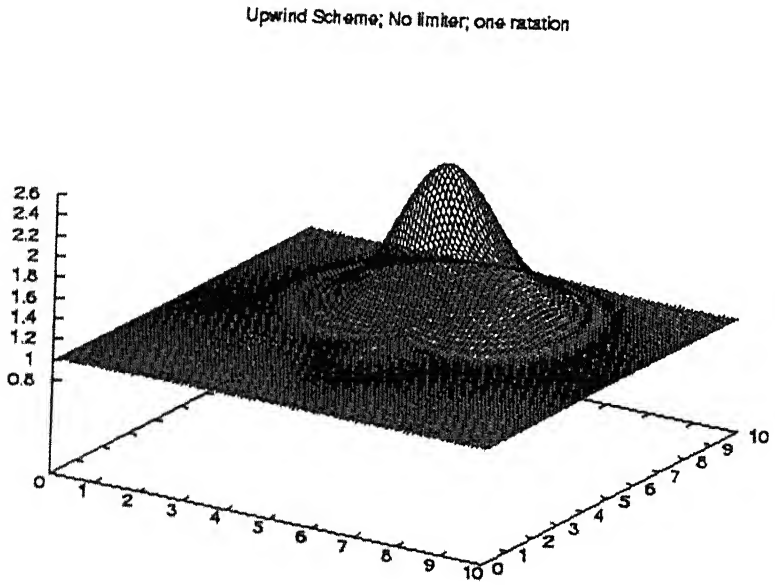

Figure 3.6 After one rotation of the cone in horizontal plane

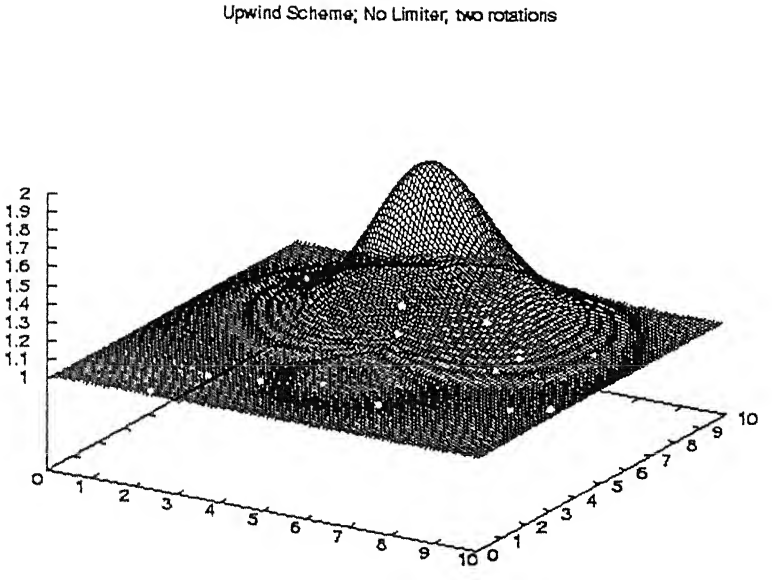

Figure 3.7 After two rotations of the cone in horizontal plane

3.2.4 Cone Test for the Limiter used in the Model

While using the combination of Van-leer limiter and Lax-Wendroff scheme, we find the following results after single and two rotations of the cone in the horizontal plane. As in the previous case, the cone has been introduced with a peak of 5 units over a base value of 1 unit. After rotation in the horizontal plane, the peak goes to 4.5 (i.e. 90% of the original) showing that little numerical diffusion is taking place. And, after two full rotations in the horizontal plane, it goes to 4.0 (i.e. 80% of the original). Furthermore, after two rotations of the cone, the peak of the cone is not going to decrease significantly, indicating that afterwards, the decrease in the peak concentration is less, and thus making the scheme to be acceptable.

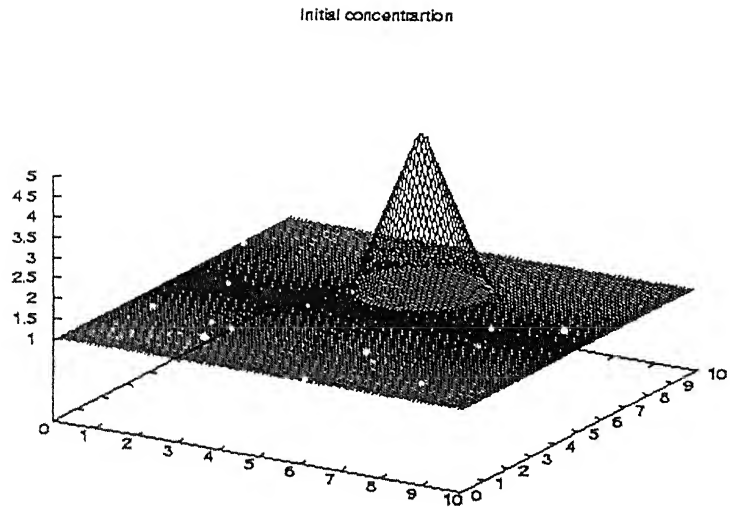

Figure 3.8 initial cone (Centre 5.0,7.5; radius 1.5 units)

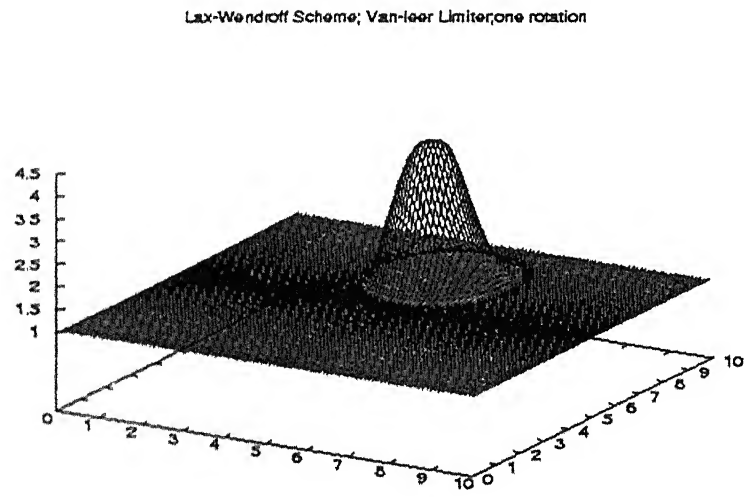

Figure 3.9 After one rotation of the cone in the horizontal plane

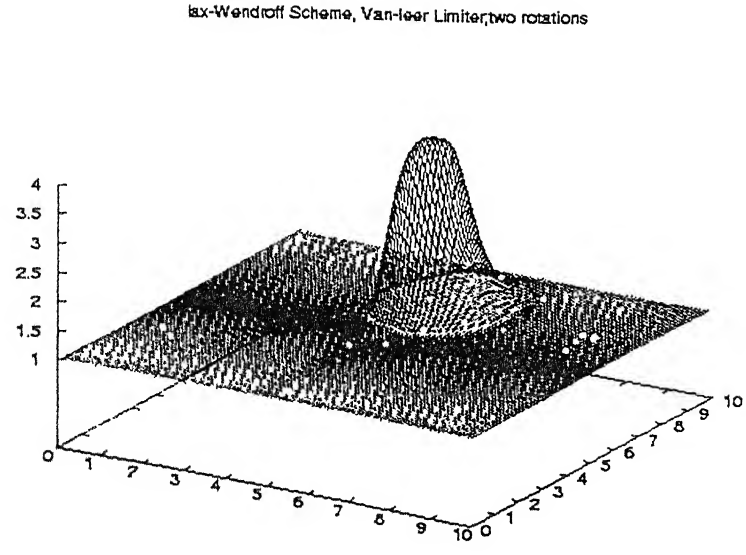

Figure 3.10 After two rotations in the horizontal plane

4. Parameters Assignment and Application of Model

This chapter presents the description of various parameters used in model application and details of field sampling .

4.1 Meteorological Parameters

4.1.1 Wind Speed and Direction

The wind speed and direction data were obtained from Weather Monitoring Station of Chandra Shekhar Azad Agricultural University (CSAAU), Kanpur and Weather Monitoring Station maintained at Environmental Engineering (EE) Laboratory, IIT Kanpur.

Measurement of wind speeds is done using a three-cup anemometer. The anemometer has a vertical axis and three cups, which captures the wind. The number of revolutions per minute is registered electronically. The anemometer is fitted with a wind vane to detect the wind direction (Envirotech Model WM-251).

The wind data are in the form of 24 hr average value at CSAAU and online continuous data of wind are available from EE laboratory, IIT Kanpur. Wind data for specific days, for which field sampling was done, were collected from these two sources.

4.1.2 Atmospheric Stability Class

Atmospheric stability classes were obtained using the wind speeds and climatic conditions (such as cloud cover, solar radiation etc.) using the insolation based technique (Seinfield, 1998). Climatic condition data were obtained from CSAAU Weather Monitoring Station.

4.1.3 Eddy Diffusivities

Eddy diffusivity in vertical direction is calculated using the wind speed and mixing height values (for unstable conditions) as per the methods presented in Appendix A.

In horizontal direction, diffusivities are taken as constant, equal in both (along the x & y) directions. Its value is taken equal to 10 m^2/s (Seinfeld, 1998).

4.2 Source Strength

4.2.1 Emission Sources

Vehicles

The primary interest of application of the model is in prediction of pollutant concentrations mainly from vehicular emissions. Emission rates have been estimated using number of vehicles and emission factors developed by Indian Institute of Petroleum (IIP). (Table 4.1.; IIP, 1982; taken from Sharma, 1999).

Sivacoumar and Thanasekaran, (2000) have proposed emission factors as a function of speed of vehicle and the same are used in calculating the emission quantities of carbon monoxide, when vehicles are in motion.

Traffic pattern for the different types of vehicles have been shown in Figures 4.1 and 4.2 at two locations, Gurdev crossing and Rawatpur crossing (Figure 4.3).It is clear from these figures that traffic density is much higher at Rawatpur than at Gurdev crossing. There are generally two peaks, in morning between 10-11 AM and in evening between 6-7 PM. Vehicle pattern shows that two wheelers are maximum in number followed by Vikram Tempos and four wheelers.This information on number of vehicles is translated into hourly emission rates at these two crossings.

It may be noted that at each of the above crossings, two receptors points have been taken to predict air concentrations (GD-R1 and GD-R2 at Gurdev crossing and RP-R1 and RP-R2 at Rawatpur crossing; Figures 4.4 and 4.5).

Table 4.1 Emission factors for different vehicles (IIP, 1982)

Vehicle Type	CO	HC	NO_x	TSP*
Two-wheelers	8.30	5.18	---	---
Cars	24.03	3.57	1.57	---
Three-wheelers	12.25	7.65	---	---
Buses (Suburban)	5.87	2.27	11.10	0.37
Buses (Urban)	4.51	1.75	8.52	0.28
Trucks	3.52	1.36	6.66	0.22
Light Commercial Vehicles	1.30	0.50	2.50	0.10

* : TSP has been taken as PM_{10} (Particulate matter less than 10 μm size)

N.B. All the values are in g/km/vehicle.

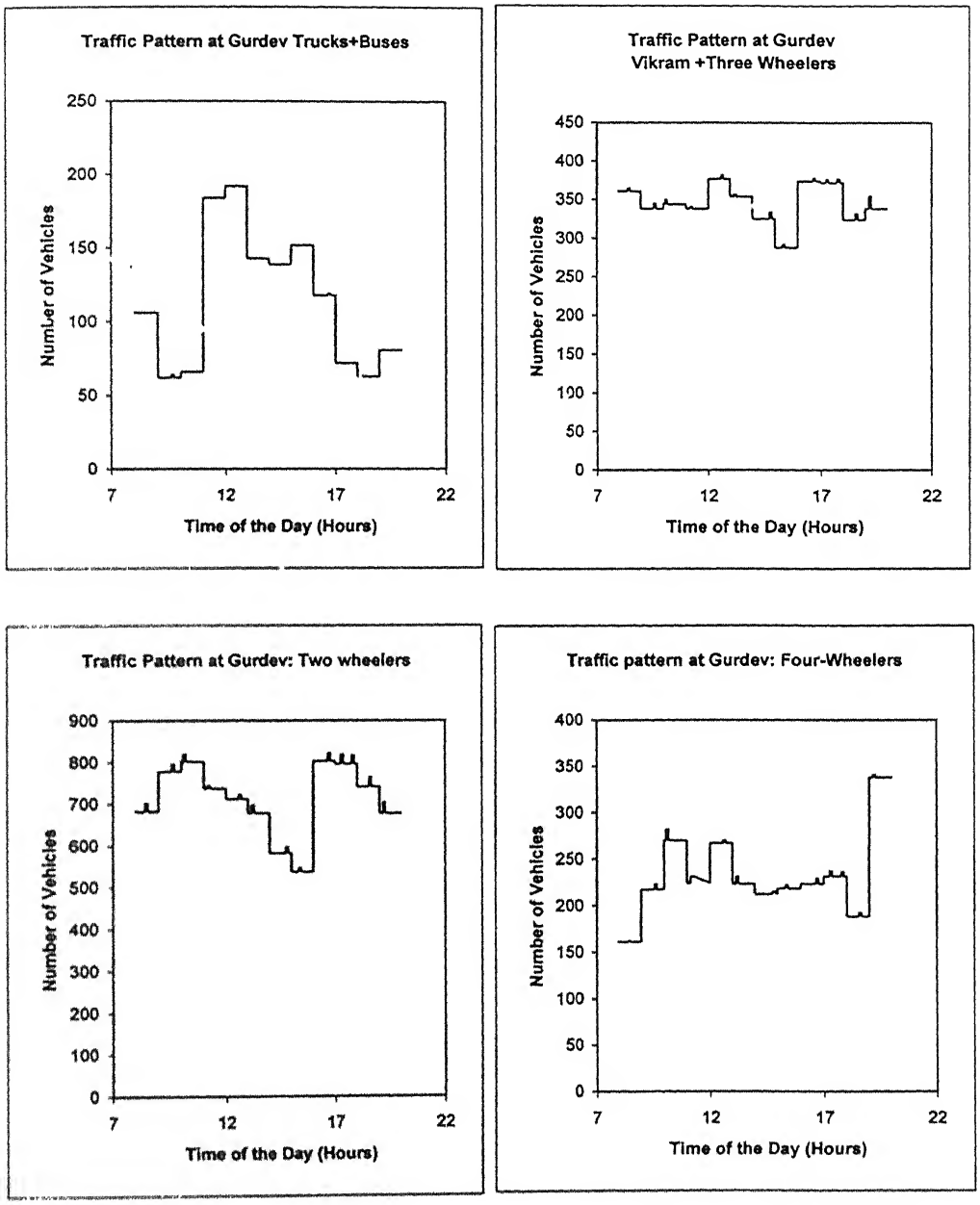

Figure 4.1 Traffic Pattern at Gurdev Crossing

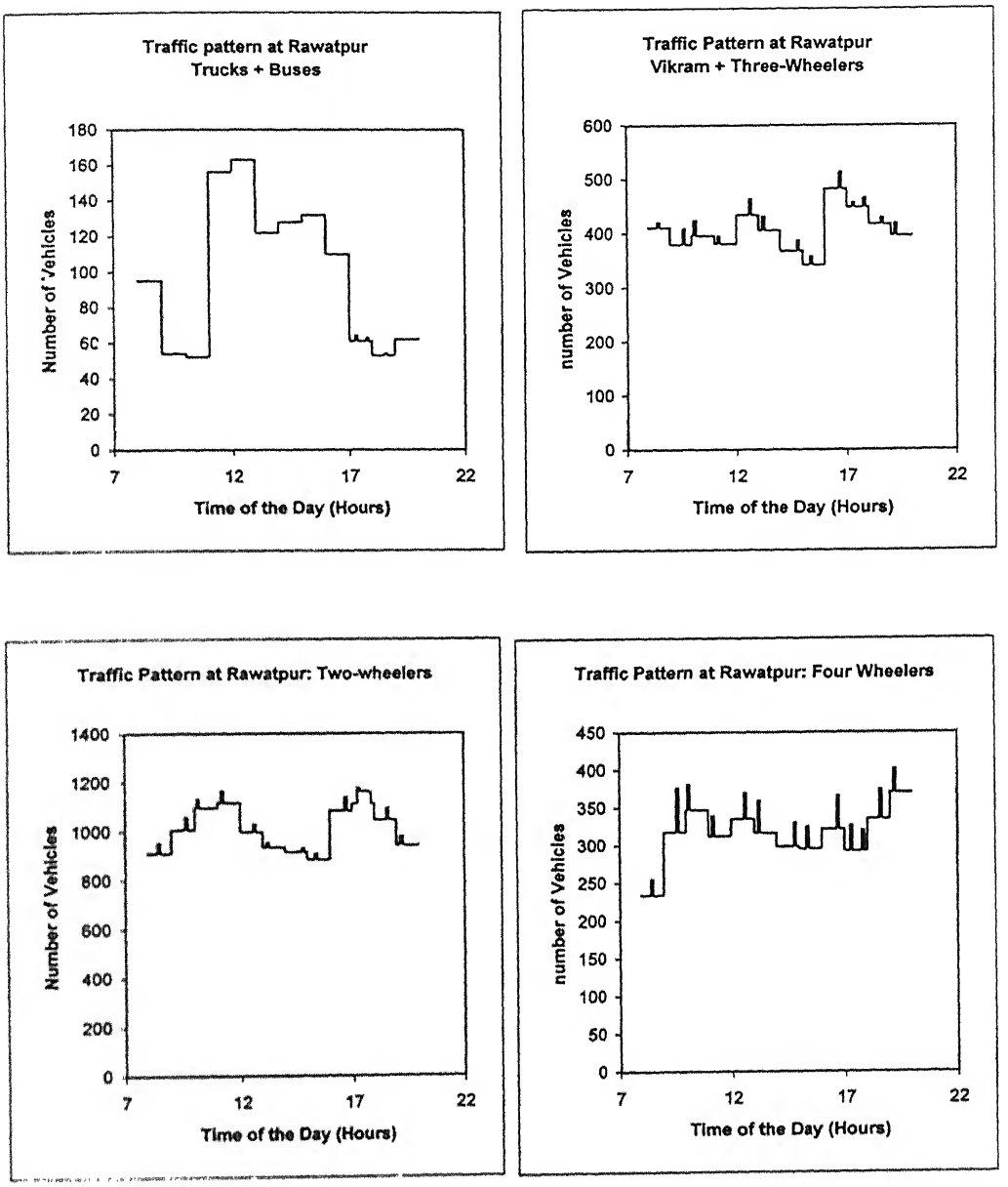

Figure 4.2 Traffic Pattern at Rawatpur Crossing

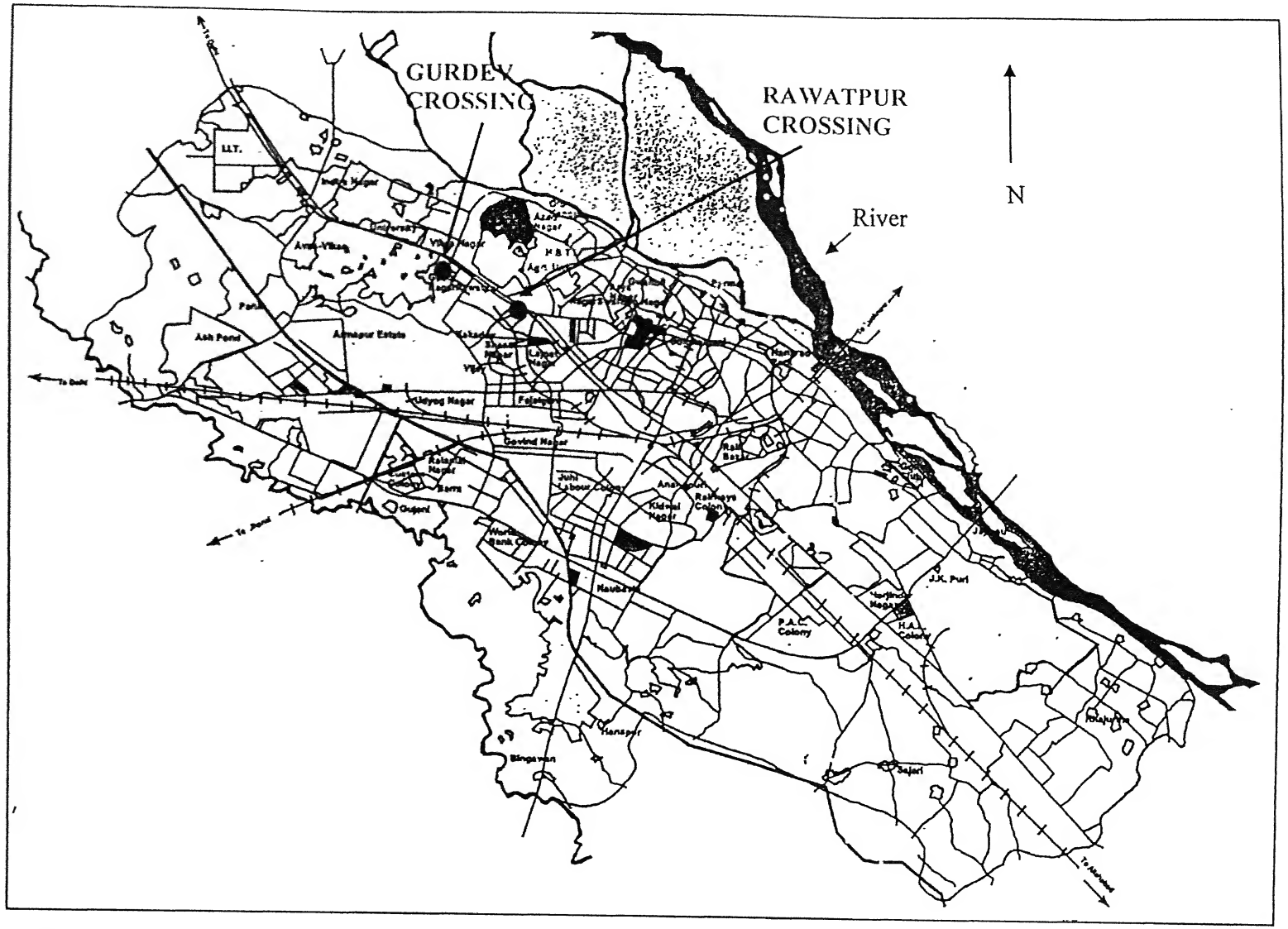

Figure 4.3 Map of Kanpur City showing the measurement site locations

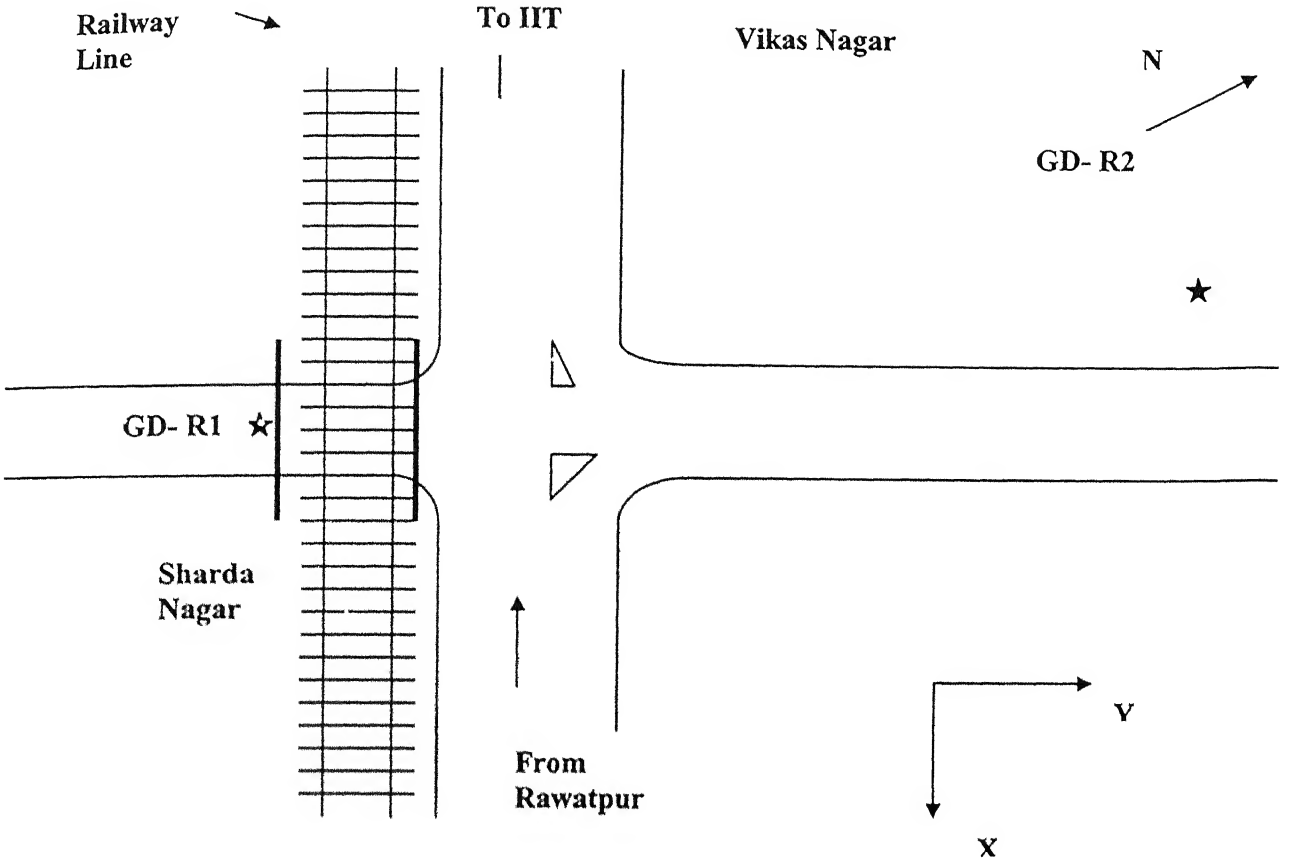

Figure 4.4 Road Layout at Gurdev Crossing with receptor locations

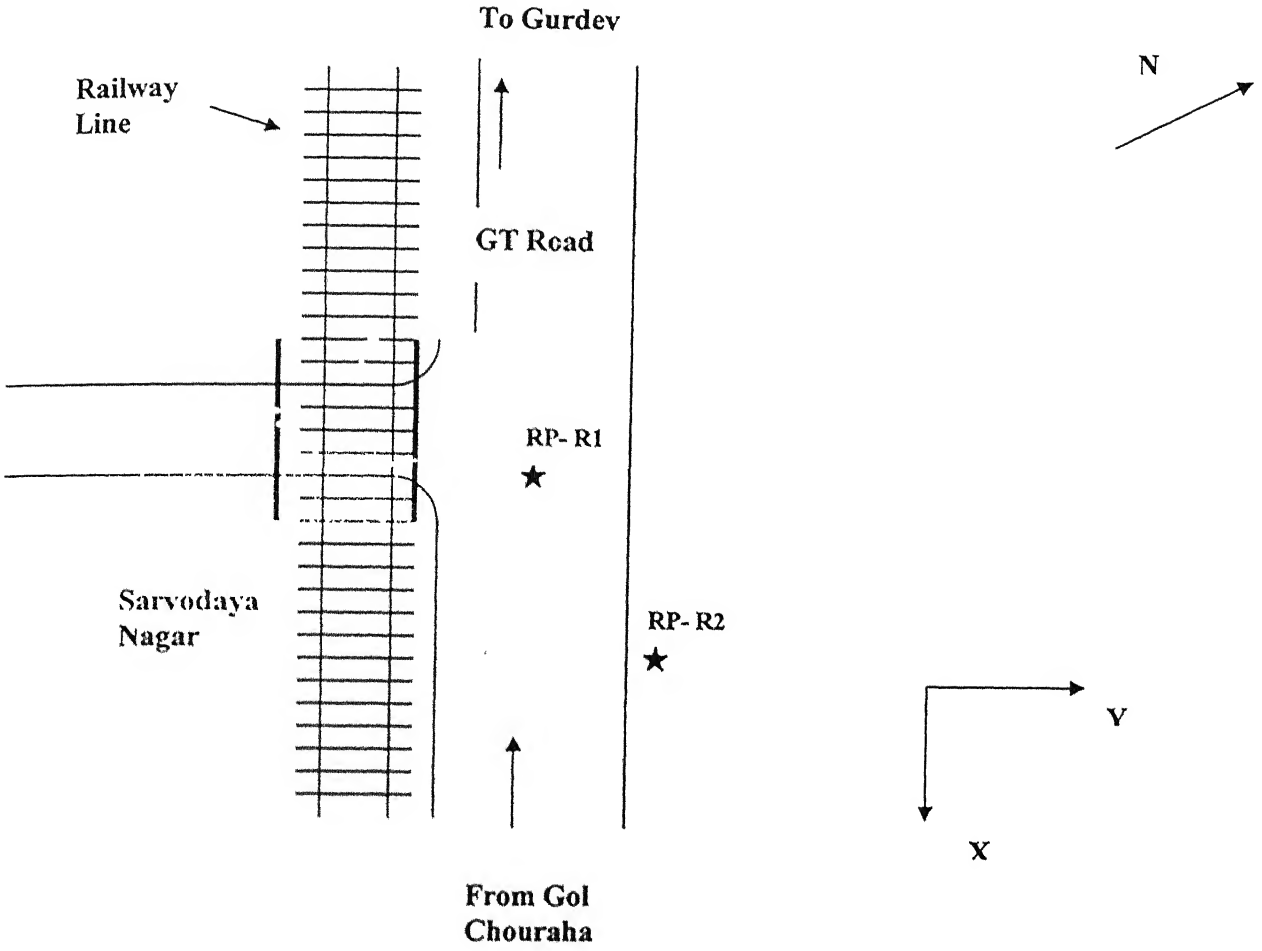

Figure 4.5 Road Layout at Rawatpur Crossing with receptor locations

4.2.2 Road Side Dust Emission

One major source of fine particulate is road dust resulting from movement of traffic. USEPA has developed generic equations to estimate particulate emissions from paved and unpaved roads depending on road conditions and weight of vehicle.

PM_{10} and $PM_{2.5}$ Emission Factor Equations

Dust emissions from paved roads have been found to vary with the silt loading present on the road surface as well as the weight of vehicles traveling on the road. For unpaved road, besides the silt content and vehicle weight, the dust emissions also vary with vehicle speed and average number of vehicle wheels.

Paved Road

Road dust emission due to traffic has been calculated using the following empirical equation (EPA-website)

$E = k^* (SL/2)^{0.65} (W/3)^{1.5} ((365-N)/365)$

where E = particulate emission, g/vkmt

k = 4.6 for PM_{10}, 1.1 for $PM_{2.5}$

SL = silt loading, g/m^2 (measured in field as 15 gm/m^2)

W = average vehicle weight, tons (taken as per actual weights)

N = number of days in year with having rain more than 2.5 cm. (taken as 40)

The derived emission factors for road dust emission corresponding to paved roads are shown in Table 4.2.

Table 4.2 Fugitive Emission Factors for road-side dust for different vehicles

Type of Vehicles	Fugitive Emission Factor (g/km)
Truck	34.825
Bus	26.492
Vikram	4.353
Two-wheeler	0.074
Three-wheeler	0.599
Four-wheeler	6.702

4.2.3 Background Pollutant Concentration

Background concentration of PM_{10} in atmosphere was taken as 60 $\mu g/m^3$ as estimated by Sharma et al. (2002) for Kanpur city.

4.3 Measurement Sites and Field Sampling

4.3.1 Site locations

The emission inventory of PM_{10} in the city of Kanpur has not been prepared. The main sources of pollutant emissions in the study area include industrial, vehicular and other combustion processes. The air pollutant emissions are from a coal-based 200 MW thermal power plant (industries) and from 250000 vehicles, which ply on the road.

Figure 4.4 shows receptor locations (GD-R1 and GD-R2), where actual sampling of PM_{10} was undertaken during the month of January 2002 using high volume sampler (Nettle,Mumbai,NPM-HVS-850).

4.4 Pollutant Parameters

In this study, only two pollutant parameters are considered for prediction of ambient air concentrations. These are:

(i) PM_{10} ; and

(ii) Carbon monoxide (CO)

Reasons for selecting these to pollutants include that PM_{10} levels are very high in the city of Kanpur (about 2-4 times higher than National Ambient Air Quality Standards) and CO is the main pollutant from automobiles.

4.5 Grid Description for Model Application

To solve equation 3.1 numerically, a three dimensional space with dimensions 500 m x 500 m x 200 m was taken and was divided in the grids 50 x 50 x 40. Thus the size of the small grid is 10 m x 10 m x 5 m.

5. Results and Discussion

5.1. Model Validation

As stated in Chapter 4 (Section 4.3), two locations (GD-R1 and GD-R2) were taken for the sampling of PM_{10} to generate the data for model validation. Table 5.1 presents the results of measured PM_{10} levels at these two locations.

Table 5.1 : Measured PM_{10} levels (8- hr average) at GD- R1 and GD- R2

Date	PM_{10} ($\mu g/m^3$), GD- R1 (8-hr average)	PM_{10} ($\mu g/m^3$), GD- R2 (8-hr average)
January 25, 2002	428	98
January 28, 2002	477	149
January 30, 2002	617	118
January 31, 2002	354	145

It is clear from Table 5.1 that as one moves away from the road, the levels of PM_{10} drop rapidly. It may be observed that measured levels of PM_{10} at both locations exceed the National Ambient Air Quality Standard of 100 $\mu g/m^3$.

It may be mentioned that it is not desirable to take a sample smaller than 8-hr duration, as accuracy of the gravimetric analysis reduces for shorter sampling. Therefore, model validation can only be done for 8-hr measured values vis-à-vis 8-hr average model-computed values. It may, however, be noted that model has the capability of predicting concentrations for very small time steps (in seconds), if desired.

Figure 5.1 shows the linear plot between measured and model-computed 8-hourly values at the two receptors considered for model validation.

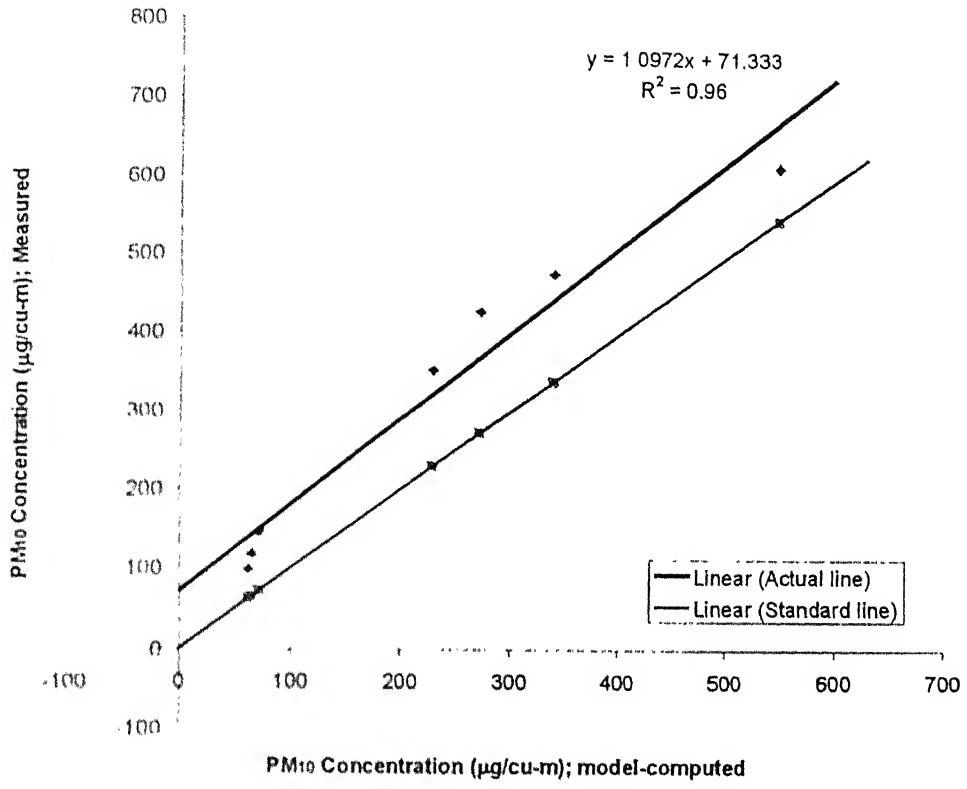

Figure 5.1 Comparison of Measured and Predicted PM_{10} Concentrations

There are several noteworthy points that can be drawn from Figure 5.1.

- The model consistently under predicts the concentration compared to the measured concentrations. In fact, this pattern of under prediction was expected. It may be noted that the model uses the emissions caused by vehicles and road dust alone, whereas the measured concentration is the resultant of the combination of emissions from several sources in the city of Kanpur.
- Figure 5.1 suggests that even if predicted value is zero (i.e. no movement of vehicles), a background level of 71.33 $\mu g/m^3$ will exist at these two locations, which can be attributed to contribution from the other sources.
- The model prediction and actual pattern of PM_{10} concentration match very well as indicated by R^2 value (= 0.96) and slope of the line (=1.0972) being close to unity. The value of R^2 is significant at 5% level of significance in a statistical sense. Therefore, it can be concluded that model adequately describes the dispersion of pollutants in urban environment

5.2 Model Application

5.2.1 Results at GD- R1 and GD-R2

Figures 5.2 and 5.3 present hourly variation in the value of PM_{10} at two receptors (GD-R1 and GD- R2) at Gurdev crossing. As expected, the predicted concentrations are higher at location GD- R1 than that at GD- R2 on both the days of prediction and this situation is true for every hour. It suggests that the impact of vehicular emission diminishes, as one moves away from the roadside. This pattern of decline in air concentration has also been found by other researchers (Harrison and Johnston, 1985; Hewitt and Rashed, 1991) for PAHs and Pb (emitted from vehicles).

It can be noted that peak hourly concentrations can be several times higher than National Ambient Air Quality Standards (i.e. 100 $\mu g/m^3$), which may cause discomfort and other health impacts to the people those are exposed for a long time to the air on the roadside.

The model results of PM_{10} concentrations follow the vehicular density for a given hour; more vehicles at the intersection, higher is the concentration.

Another interesting fact, which emerges out from the comparison of Figures 5.2 and 5.3 is that PM_{10} level shooted up on January 28, 2002 compared to January 25, 2002 (in spite of same emission rate). To understand this variation, one need to examine the meteorological parameters such as values of average wind speed (U) and $\Delta\theta$ (difference in wind direction and the direction of receptor, in degrees). As the wind speed increases, the concentration comes down due to dilution effect and as $\Delta\theta$ becomes small, it suggests that receptor is coming in the downwind direction of emissions and will receive more pollution. In case of January 28, 2002 results for GD- R1, U and $\Delta\theta$, both have decreased (compared to values on January 25, 2002) resulting in high level of PM_{10} at GD- R1.
The influence of meteorology can also be seen at GD- R2 to a lesser extent, while comparing the concentrations on January 25 and 28, 2002.

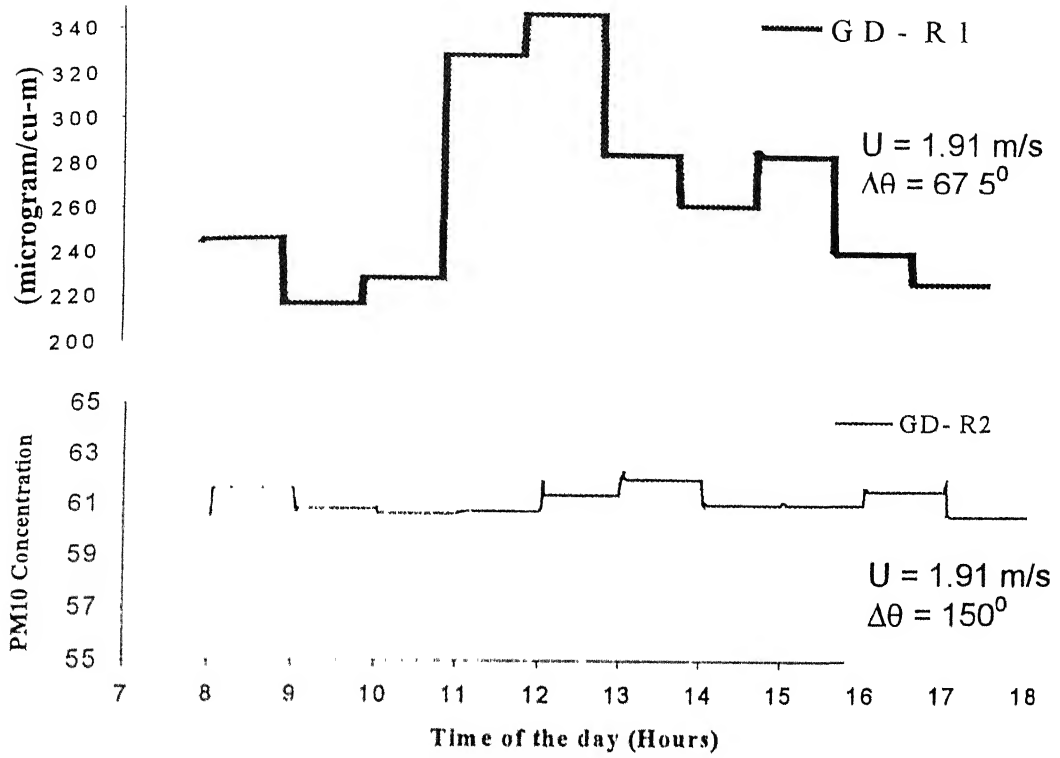

Figure 5.2 Diurnal variation in PM_{10} Concentration as predicted by the Numerical Model. (25th Jan 2002)
(U → Average wind speed, Δ0 → Dir. of wind – dir. of receptor)

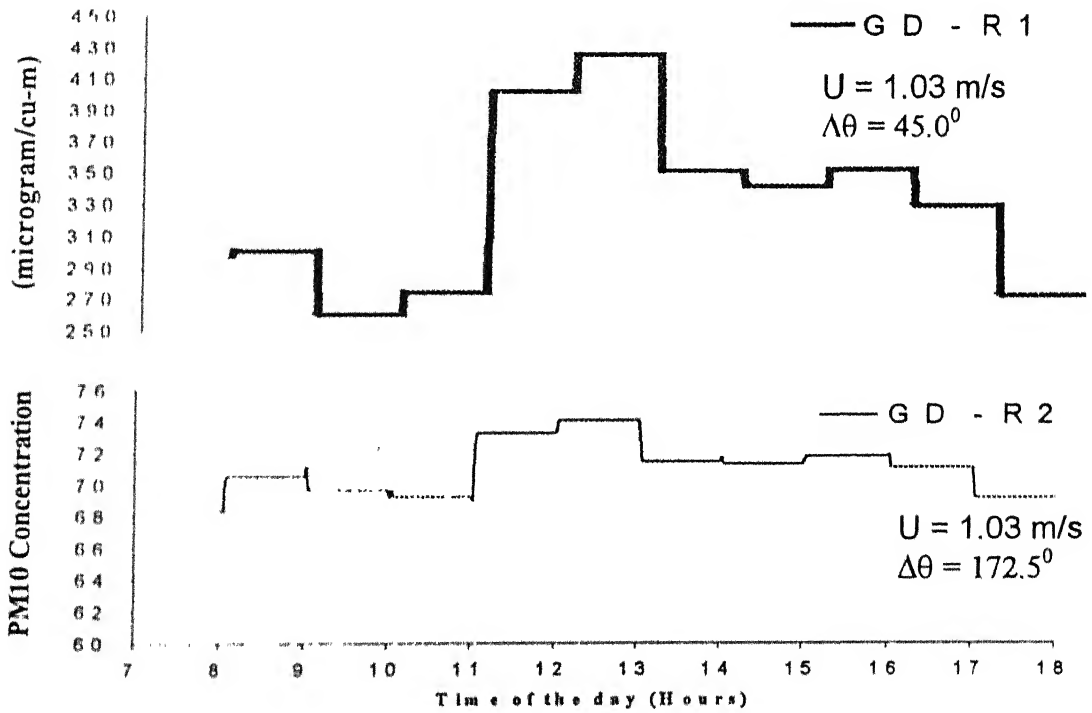

Figure 5.3 Diurnal variation in PM_{10} Concentration as predicted by the Numerical Model. (28th Jan 2002)
(U → Average wind speed, Δθ → Dir. of wind – dir. of receptor)

5.2.2 Results at RP-R1 and RP-R2

At these two locations of Rawatpur crossing, the traffic density is much higher than at Gurdev crossing (see Figures 4.1 and 4.2). At this crossing also, two receptor locations RP- R1 (close to the intersection) and RP- R2 (away from the intersection) are taken for prediction of concentration. Model predictions of concentrations of two pollutants, CO and PM_{10} have been carried out for April 10, 2002.

Attempts have also been made to compare the results of the developed model with that of ISCST 3 model of USEPA (USPEA,1995). Figures 5.4 and 5.5 show the comparisons made between the predicted values of Carbon monoxide at receptor locations RP- R1 and RP- R2 using the developed numerical model and ISCST 3 model.

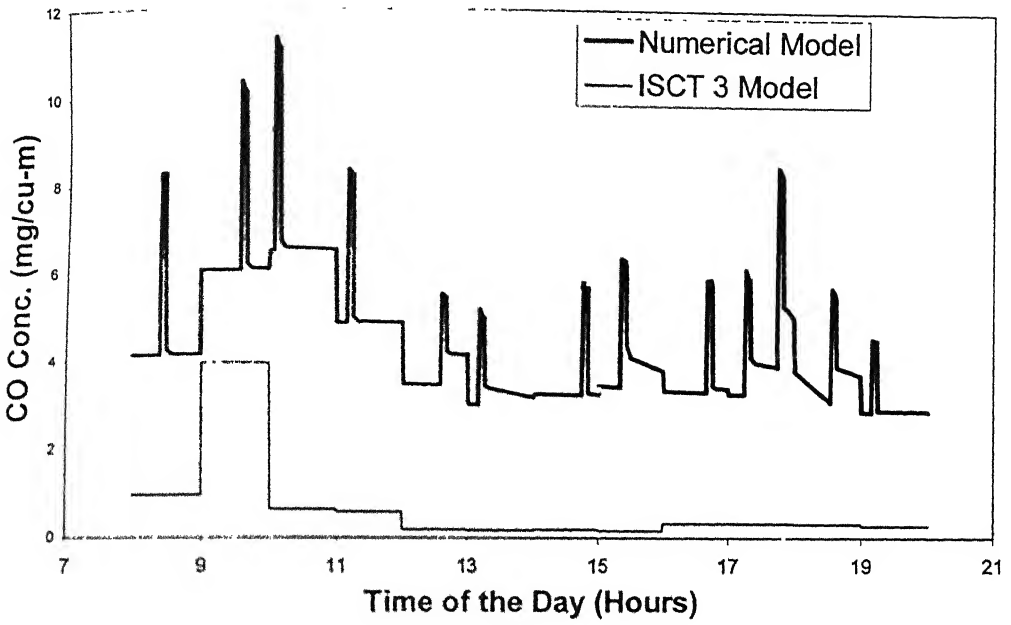

Figure 5.4 Comparison of CO concentration at RP- R1 using the Numerical Model and ISCT 3 Model (April 10, 2002)

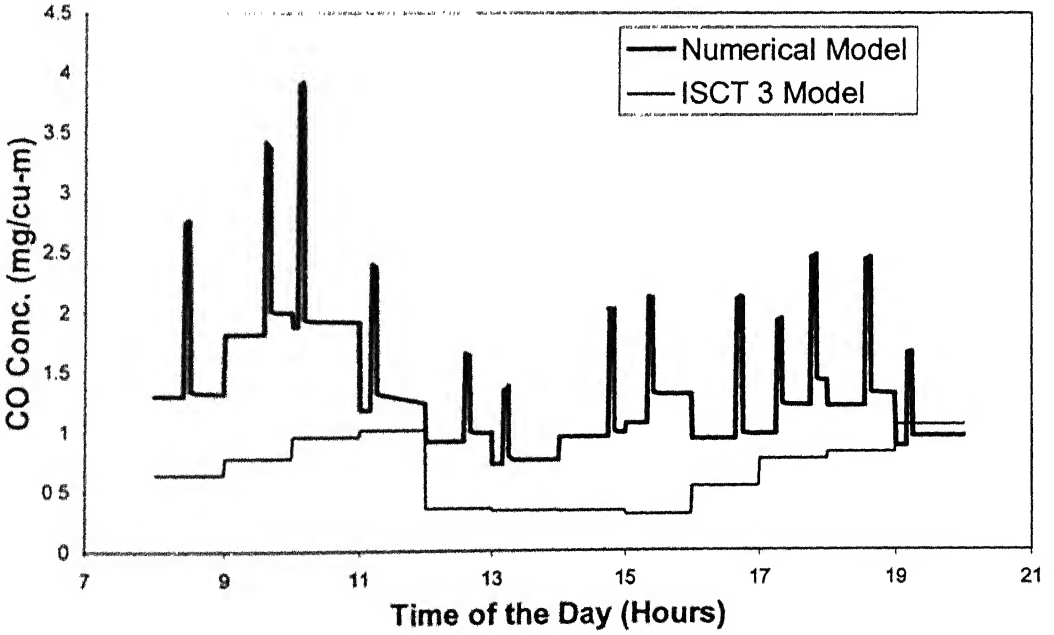

Figure 5.5 Comparison of CO concentration at RP- R2 using the Numerical Model and ISCT 3 Model (April 10, 2002)

It can be observed from the Figures 5.4 and 5.5 that the CO concentration values obtained using the numerical model is comparatively higher than that of ISCST 3 model. The concentration values are in the range of 1-11 mg/m^3 .The range is comparable to 8 hr CO concentration in Delhi, i.e 5 mg/m^3 (CPCB,2000).The sharp peaks in the results of numerical model is because of the fact that the gates of level crossing were closed due to arrival of trains. When gates are closed there is considerable increase in traffic (see Figure 4.2), which causes the consequent increase in the pollutant level. This pattern of sharp increase cannot be obtained using the Gaussian models (e.g. ISCST 3 model). Further one can get an idea that the numerical model-predicted values are much higher than concentrations predicted by ISCST 3 model. Since, it was found that numerical model under predicts (see section on model validation), it is reasonable to conclude that the developed model perform better than the ISCST 3 in the present situation with the advantage of estimation of short-term peak concentrations.

5.2.3 Prediction of PM10 Concentration at RP- R1 and RP- R2

The numerical model predicted values at the locations RP- R1 and RP- R2 for PM_{10} concentrations have been shown in Figure 5.6.

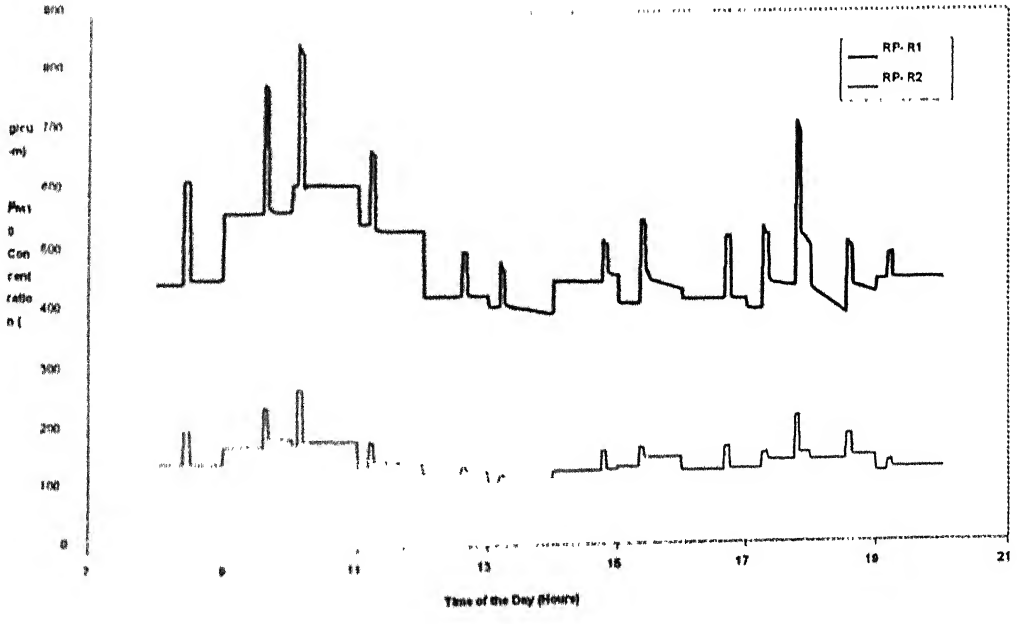

Figure 5.6 Numerical Model Predicted PM_{10} values at RP- R1 and RP- R2

It can be observed from Figure 5.6, that the PM_{10} levels at the location RP- R1 is higher than that at RP- R2 because RP-R1 is nearer to the intersection and receives more pollution.

The PM_{10} concentration at both the receptors exceed the National Ambient Air Quality Standard of 100 $\mu g/m^3$.While the average concentration of PM_{10} is 450-500 $\mu g/m^3$, the short- term peaks may even exceed the value of 800 $\mu g/m^3$ of PM_{10}, which is matter of concern for public health.

6. Conclusions

The following conclusions can be drawn from present study

The developed numerical model can capture the short-term peaks of air pollutant concentration arising due to unsteady urban conditions prevalent in city of Kanpur due to criss-cross network of road and railways. The model results clearly show that even though number of vehicles in the city of Kanpur is much less compared to large city like Delhi, pollutant concentration in Kanpur can be much higher due to traffic congestion and poor planning.

In terms of numeric concentration, model suggests that carbon monoxide concentration exceed the national ambient air quality standard by a factor of 2 at Rawatpur crossing Similarly, PM_{10} levels also exceed the standard by a factor of 4-6 on the two crossings studied in Kanpur city.

7. Scope for Future Work

There is an urgent need for good quality experimental data, which should be specifically produced for further model validation and evaluation purposes.

The present model does not incorporate reactions of chemical species. A more detailed output can be obtained after consideration is made for the formation and removal of pollutant species of interest in the atmosphere.

The model should be used to develop pollution control strategies for various crossings in the city of Kanpur.

REFERENCES

Budianski, S., 1980. Dispersion Modelling. Environmental Science and Technology 14, 370-374.

Chock, D.P., 1978. A Simple Line-Source Model for Dispersion Near Roadways. Atmospheric Environment 12, 823-829.

Clappier, A., 1998. A correction Method for Use in Multidimensional Time-Splitting Advection Algorithms: Application to Two- and Three-Dimensional Transport. Monthly Weather Review 126, 232-242.

CPCB (2000). Air Quality Status and Trends in India. Report No. NAAQMS/14/1999-2000, Delhi.

Dobbins, R.A. (1979) Atmospheric Motion and Air pollution. John Wiley & Sons, Inc., New York. Pp 251-255.

EPA website. www.epa.gov/scram001/7thconf/iseprime/evalrpt.pdf

Goyal, P., Rama Krishna, T.V.B.P.S., 1999. A Line Source Model for Delhi. Transportation Research Part D 4, 241-249.

Harrison, R.A. and Johnston, W.R., 1985. Deposition Flux of lead, Copper and PAHs on the verge of Motor Highway. Science of Total Environment 46, 121-125.

Hewitt, A.N. and Rashed, M.B., 1991. The Deposition of Selected Pollutants Adjacent to a Major Rural Highway. Atmospheric Environment 25A, 979-983.

Kukkonen, J., Harkonen, J., Walden, J., Karppinen, A., Lusa, K., 2001. Evaluation of the CAR-FMI Model Against Measurement Near a Major Road. Atmospheric Environment 35, 949-960.

Luhar, A.K., Patil, R.S., 1989. A general Finite Line Source Model for Vehicular Pollution Prediction. Atmospheric Environment 23(3), 555-562.

Peterson, W.B. (1980). User's Guide for HIWAY- 2, Highway Air Pollution Model, EPA- 600/8-80-018.

Pundir, B.P., Jain, A. K., Gogia, D. K., 1994. Vehicles Emissions and Control Perspectives in India-A State-of-the-Art Report. Indian Institute of Petroleum, Dehradun.

Seinfeld, J.H., Pandis, S.N. (1998). Atmospheric Chemistry and Physics: From Air Pollution to Climate Change. John Wiley & Sons, Inc., New York.
Sharma, M. 1999. Short- term course on Air Quality monitoring and Management. Department of Civil Engineering, IIT Kanpur.

Sharma, M., Kiran, Y.N.V.M., Shandilya, K. (2002). Contribution of Soil to PM_{10} and Modelling of Atmospheric Sulphate. Submitted to Journal of Air and Waste Management.

Sivacoumar, R., Thanasekaran, K., 2000. Emission Factors and Emission Estimation for Indian Vehicles-A Case Study. Journal of Institution of Engineers: Environmental Engineering division 9, 28-31.

Srivastava, R.K., McRae, D.S., Odman, M.T., 2000.An Adaptive Grid Algorithm for Air-Quality Modelling. Journal of Computational Physics 165, 437-472.
Thomas, J.W.(1999). Numerical Partial differential Equations: Conservation Laws and Elliptic Equations. Springer-Verley New York, Inc. pp 204-215,269-284.
Tomlin, A.S., Ghorai, S., Hart, G., Berzins, M., 2000. 3-D Multi-Scale Air pollution Modelling using Adaptive Unstructured Meshes. Environmental Modelling and Software 15, 681-692.

USEPA(1995). Industrial Source Complex(ISCST3)Model. Office of Air Quality Planning and standards Emissions Monitoring and Analysis Division. Research Triangle Park,North Carotina 27711.

APPENDIX A

Wind Speed Variation and Eddy Diffusivity

Variation of Wind with Height in the Atmosphere

The atmosphere near the surface of the earth can be divided into three layers—the free atmosphere, the Ekman layer, and the surface layer. The Ekman layer extends to a height of from 300 to 500 m depending upon the type of terrain, with the greater thickness corresponding to the more disturbed terrain.

The layer immediately adjacent to the surface, typically upto 30 to 50 m from the ground, is called the surface layer. Within this layer, the vertical turbulent fluxes of momentum and heat are assumed constant with respect to height, and indeed they define the extent of this region.

Considering two-dimensional turbulent flow of air in the surface layer parallel to the ground at a height z_3, the wind speed u (z_3) can be given by,

$$\frac{u(z_3)}{u_*} = \frac{1}{\kappa} \ln \frac{z_3}{z_0} \qquad z_3 \geq z_0 \qquad (A.1)$$

where κ is a constant proportionality factor with the experimental value of 0.4 and z_0 is called the roughness length and values of z_0 for typical surfaces are given in table 1.1.

Table A.1 Roughness Lengths for Various Surfaces (Seinfeld, 1998)

Surface	Z_0 (m)
Very smooth (ice, mud flats)	10^{-5}
Snow	10^{-3}
Smooth sea	10^{-3}
Level desert	10^{-3}
Lawn	10^{-2}
Uncut grass	0.05
Fully grown root crops	0.1
Tree covered	1
Low density residential	2

Of the three parameters κ, z_0 and u_* mentioned above, z_0 is the property of the roughness. To calculate the value of u* at different depths, wind speed is measured at some convenient height, say z. Then equation (A.1) can be used to calculate the value of u* and subsequent specification of wind speeds at all values of heights.

The equation (A.1) corresponds to neutral weather conditions. For stable and unstable weather conditions, we can use the equation

$$\frac{u(z_3)}{u^*} =$$

$$\begin{cases} \dfrac{1}{\kappa}\left[\ln\left(\dfrac{z_3}{z_0}\right) + \dfrac{4.7}{L}(z_3 - z_0)\right] & \textit{stable} \\ \dfrac{1}{\kappa}\left\{\ln\left(\dfrac{z_3}{z_0}\right) + \ln\left[\dfrac{(\eta_0^2+1)(\eta_0+1)^2}{(\eta_r^2+1)(\eta_r+1)^2}\right] + 2\left(\tan^{-1}\eta_r - \tan^{-1}\eta_0\right)\right. & \textit{unstable} \end{cases} \qquad (A.2)$$

where η_r and η_0 are given by

$$\eta_r = \left[1 - 15\frac{z_3}{L}\right]^{1/4} \qquad \text{and} \qquad \eta_0 = \left[1 - 15\frac{z_0}{L}\right]^{1/4}$$

L, called Monin-Obukhov length is not a parameter that is routinely measured. It is the height above the ground at which the production of turbulence by both mechanical and buoyancy forces is equal. It provides a measure of the stability of the surface layer. To fulfil the need, we can approximate the Golder's (1972) plot between the Pasquill stability classes, the roughness length z_0 and L, by the correlation

$$L = (a + b \log z_0)^{-1} \qquad (A.3)$$

The values of a and b have been listed in Table A.2.

Determination of Pasquill stability classes is made as per Table A.3.

Table A.2 Coefficients for straight-line approximation to Golder's plots as a function of stability classes (Seinfeld, 1998)

	Pasquill Stability Class	Coefficients	
		a	b
Extremely unstable	A	-0.096	0.029
Moderately unstable	B	-0.037	0.029
Slightly unstable	C	-0.002	0.018
Neutral	D	0	0
Slightly stable	E	+0.004	-0.018
Moderately stable	F	+0.035	-0.036

Table A.3 Estimation of Pasquill Stability Classes (Seinfeld, 1998)

Surface Wind Speed at 10m (m/s)	Solar Radiation			Night time cloud Cover fraction	
	Strong	Moderate	Slight	>= 4/8	<= 3/8
<2	A	A-B	B	----	----
2-3	A-B	B	C	E	F
3-5	B	B-C	C	D	E
5-6	C	C-D	D	D	D
>6	C	D	D	D	D

Eddy Diffusivity Coefficients

Horizontal Eddy Diffusivity Coefficient K_{xx} and K_{yy}:

Equation (1.1.1) shows that the turbulent diffusivity has three components, but the more careful formulation demonstrates that it is a second order tensor with nine components. Thus, for example, the x- component of the Reynolds dispersion terms are more rigorously given by

$$K_{xx}\frac{\partial c}{\partial x} + K_{xy}\frac{\partial c}{\partial y} + K_{xz}\frac{\partial c}{\partial z}$$

However, no information on the off-diagonal terms, such as K_{xy} and K_{xz} are available, and it is customary to assume that they are zero. Furthermore, we usually assume that the horizontal eddy diffusivities are equal, $K_{xx} = K_{yy}$. The equation for turbulent dispersion then contains only K_{xx}, K_{yy} and K_{zz} terms.

For a range of typical meteorological conditions, we find diffusivities under unstable conditions in the order of (50-100 m^2/s).

Vertical Eddy diffusion Coefficient K_{zz}:

The expressions available for K_{zz} are based on Monin-Obukhov similarity theory coupled with observational or computationally generated data. It is best to organize the expressions according to the type of stability.

Since we generally need expressions for K_{zz} that extend vertically beyond the surface layer, we should consider some available correlations for the entire Ekman Layer.

Unstable conditions:

When turbulence in the atmospheric boundary layer is maintained largely by buoyant production, the boundary layer is said to be in a convective state. The source of buoyancy is the upward heat flux originating from the ground heated by solar radiation. Convective turbulence is relatively vigorous and causes rapid vertical mixing in the atmospheric boundary layer.

In the unstable weather conditions, there is usually an inversion base height at $z = z_i$ that defines the extent of the mixed layer. The two parameters that are key in determining Kzz are the convective velocity scale w_* and z_i. An empirical

expression for Kzz under unstable conditions, using the numerical turbulence model of Deardorff (1970) is as follows:

$$\frac{K_{zz}}{w_* z_i} = \begin{cases} 2.5\left(\kappa\frac{z}{z_i}\right)^{4/3}\left(1-15\frac{z}{L}\right)^{1/4} & 0 \le \frac{z}{z_i} < 0.05 \\ 0.021 + 0.408\frac{z}{z_i} + \left(\frac{z}{z_i}\right)^2 - 4.096\left(\frac{z}{z_i}\right)^3 + 2.560\left(\frac{z}{z_i}\right)^4 & 0.05 \le \frac{z}{z_i} \le 0.6 \\ 0.2\exp\left[6 - 10\left(\frac{z}{z_i}\right)\right] & 0.6 \le \frac{z}{z_i} \le 1.1 \\ 0.0013 & \frac{z}{z_i} > 1.1 \end{cases} \qquad (A.4)$$

Neutral Conditions:

The following relationship (Shir, 1973) for Kzz can be used successfully under neutral conditions:

$$K_{zz} = \kappa u_* z \exp\left(-\frac{8fz}{u_*}\right) \qquad (A.5)$$

where, f is the coriolis parameter.

Stable Conditions:

Under stable conditions, the appropriate characteristic vertical length-scale is L. Businger and Arya (1974) proposed a modification of surface layer similarity theory to extend its vertical range of applicability.

$$K_{zz} = \frac{\kappa u_* z}{0.74 + 4.7(z/L)} \exp\left(-\frac{8fz}{u_*}\right) \qquad (A.6)$$

APPENDIX B

Table B1: Traffic Count at Gurdev Crossing (along G.T. road)

Time	Trucks	Buses	Vikrams	2-Wheelers	3-Wheelers	4-Wheelers (Cars etc.)	Tractors
8 a.m. - 9 a.m.	80	26	352	682	9	161	3
9 a.m. - 10 a.m.	48	14	315	778	23	217	8
10 a.m. - 11 a.m.	46	20	323	802	21	270	9
11 a.m - 12 noon	145	39	321	737	17	224	12
12 noon - 1 p.m.	140	52	362	712	15	267	11
1 p.m. - 2p.m.	105	38	333	678	21	223	12
2 p.m. - 3 p.m.	113	26	289	582	36	212	10
3 p.m - 4 p.m.	118	34	256	537	32	218	6
4 p.m. - 5 p.m.	95	23	346	803	28	223	8
5 p.m. - 6 p.m.	57	15	331	793	41	231	10
6 p.m. - 7 p.m.	49	14	289	741	35	188	7
7 p.m. - 8 p.m.	62	19	322	677	16	338	12

Table B2: Traffic Count at Rawatpur Crossing (along G.T. road)

Time	Trucks	Buses	Vikrams	2-Wheelers	3-Wheelers	4-Wheelers (Cars etc.)	Tractors
8 a.m. - 9 a.m.	74	21	398	910	13	234	4
9 a.m. - 10 a.m.	42	12	342	1006	38	318	8
10 a.m. - 11 a.m.	35	17	359	1096	37	347	7
11 a.m. - 12 noon	113	43	353	1117	28	312	15
12 noon - 1 p.m.	115	48	402	997	32	335	8
1 p.m. - 2p.m.	88	34	367	934	39	316	15
2 p.m. - 3 p.m.	96	32	325	915	43	298	12
3 p.m. - 4 p.m.	86	46	290	884	52	295	7
4 p.m. - 5 p.m.	83	27	436	1084	46	321	7
5 p.m. - 6 p.m.	45	16	387	1113	61	292	8
6 p.m. - 7 p.m.	40	13	386	1046	31	335	7
7 p.m.- 8 p.m.	48	14	378	942	18	370	11

Table B3: Traffic Count at Rawatpur Crossing (on the road orthogonal to G.T. road and towards Kakadev)

Time	Trucks	Buses	Vikrams	2-Wheelers	3-Wheelers	4-Wheelers (Cars etc.)	Tractors	Train Arrival Time
8 a.m. - 9 a.m.	4	17	67 (6)	543 (42)	23 (4)	245 (21)	12	8:25 a.m.
9 a.m. - 10 a.m.	0	23	156 (13)	602 (52)	45 (16)	267 (58)	3	9:35 a.m.
10 a.m. - 11 a.m.	5	13	114 (10)	518 (38)	65 (18)	214 (34)	5	10:05 a.m.
11 a.m. - 12 noon	2	7	79 (7)	556 (49)	37 (7)	314 (27)	8	11:10 a.m.
12 noon - 1 p.m.	7	6	84 (23)	456 (32)	48 (6)	308 (35)	4	12:35 p.m.
1 p.m. - 2p.m.	5	12	34 (21)	423 (19)	22 (4)	279 (43)	6	1:10 p.m.
2 p.m. - 3 p.m.	4	16	23 (13)	487(17)	37 (6)	268 (32)	12	2:45 p.m.
3 p.m. - 4 p.m.	7	6	56 (15)	378 (24)	19	231 (29)	7	3:20 p.m.
4 p.m. - 5 p.m.	3	8	112 (30)	627(55)	32 (1)	257 (45)	22	4:40 p.m.
5 p.m. - 6 p.m.	8	20 (3)(2)	56 (6)(16)	540 (63)(45)	16 (2)(1)	298 (34)(28)	4	5:15 p.m. and 5:45 p.m.
6 p.m. - 7 p.m.	3	8 (1)	106 (12)	411 (48)	15	304 (39)	9	6:33 p.m.
7 p.m.- 8 p.m.	4	5	121(18)	467(36)	18 (4)	288 (32)	7	7:10 p.m.

N.B. Values in the parentheses show the vehicles waiting on either side of the level crossings at the time of arrival of the train.

Table B4: Traffic Count at Gurdev Crossing (on the road orthogonal to G.T. road and towards Zoo)

Time	Trucks	Buses	Vikrams	2-Wheelers	3-Wheelers	4-Wheelers (Cars etc.)	Tractors	Train arrival Time
8 a.m. - 9 a.m.	0	3	19 (2)	326 (20)	11 (2)	122 (1)	3	8:40 a.m.
9 a.m. - 10 a.m.	0	14 (2)	32 (4)	346 (18)	22 (3)	178 (6)	1	9:15 a.m.
10 a.m. - 11 a.m.	1	12	26 (3)	378 (12)	29 (3)	134 (12))	2	10:15 a.m.
11 a.m. - 12 noon	0	2	25 (3)	288 (8)	20	98 (7)	5	11:17 a.m.
12 noon - 1 p.m.	0	8	12 (5)	312 (11)	14	84 (3)	2	12:45 p.m.
1 p.m. - 2p.m.	0	7	8 (3)	257 (20)	16	86 (8)	2	1:05 p.m.
2 p.m. - 3 p.m.	2	5	16 (7)	287 (15)	21 (2)	102 (3)	4	2:40 p.m.
3 p.m. - 4 p.m.	0	6	19 (4)	312 (9)	17	116 (4)	3	3:30 p.m.
4 p.m. - 5 p.m.	0	13 (1)	23 (5)	320 (19)	18	92 (6)	7	4:33 p.m.
5 p.m. - 6 p.m.	0	6	26 (4)(5)	285 (22)(18)	9	120 (6)(5)	2	5:25 p.m. and 5:52 p.m.
6 p.m. - 7 p.m.	0	3	22 (8)	338 (24)	10	128 (4)	0	6:40 p.m.
7 p.m. - 8 p.m.	0	4	28 (12)	347 (27)	16 (4)	108 (3)	1	7:05 p.m.